ISSN 1054-660X, Laser Physics, 2010, Vol. 20, No. 5, pp. 1101–1106.

Air Filaments and Vacuum[1]

J.-C. Diels[a], J. Yeak[a], D. Mirell[a], R. Fuentes[b, c], S. Rostami[a], D. Faccio[d], and P. di Trapani[d]

[a] *The University of New Mexico, Department of Physics, Albuquerque, NM 87131, USA*
[b] *Center for Optics and Photonics, Universidad de Concepción, Casilla C4016, Conceptión, Chile*
[c] *Departamento de Fisica, Universidad de Concepción, Casilla C-160, Concepción, Chile*
[d] *University of Insubria at Como, Corao, Italy*
**e-mail: jcdiels@unm.edu*

Received November 2, 2009; in final form, November 24, 2009; published online April 2, 2010

Abstract—The use of a new diagnostic tool combined with an aerodynamic window forming a boundary between vacuum and air provides differentiation between the "preparation phase" and the "confinement phase" of filaments.

DOI: 10.1134/S1054660X10090379

1. INTRODUCTION

"Filamentation" is a phenomenon that was discovered in 1994 and 1995 with IR [1] and UV [2] pulses, respectively. After one and a half decades of research, the number of potential applications has increased dramatically, and while there is an equally large number of models and theories, no general understanding exists. It is difficult to gain a clear understanding of a phenomenon like filamentation, where there is an obscure curtain of the order of a meter that separates the prepared initial conditions for a filament from the observed filament itself. The thrust of this paper is to present experimental evidence that has never been accessed before. An aerodynamic window separating vacuum and atmosphere with a thin sheet of supersonic air-flow, makes it possible for the first time to compare filament prepared the traditional way in air, or from a 200 μm beam waist created in vacuum. It is therefore possible for the first time to distinguish between phenomena resulting from the "preparation phase" of filaments (self-focusing of a macroscopic beam in air) and the "waveguiding phase" (dynamic balance between focusing and defocusing). This paper begins with a brief review of two main concepts about the nature of filaments: The generation of a self-confined beam due to the nonlinearities of air with a plasma-like behavior; and the generation of a "Bessel beam" that results from the beam preparation in a pre-filament phase. Next, we present some unique tools that have enabled the experiments on filaments to be performed with much better control than what has been achieved previously. These tools are: (i) a linear attenuator of a factor of 10^{-8} capable of handling the high peak intensities of IR and UV filaments; and (ii) an aerodynamic window that has enabled us to start filaments from any set of initial conditions, in particular a 200 μm beam waist prepared in vacuum. Experiments comparing the filaments created in the traditional fashion with those created from a pre-defined beam waist in vacuum through an aerodynamic window have shown surprising differences.

[1] The article is published in the original.

2. SOME ELEMENTARY CONSIDERATIONS

There has been a considerable number of models and numerical simulations on filaments. Several review papers have been published on *comprehensive* models of filamentation [3–6] including dispersion, diffraction, instantaneous and retarded nonlinearities, correction to slowly varying envelope approximation, etc. ... . The shear number of competing phenomena and parameters involved makes it difficult to extract a physical picture of the phenomenon of filamentation. Two distinct physical pictures have been proposed to explain the confined intensity distribution of filaments. The oldest description is that of a plasma channel: filaments are formed in air when the self-focusing due to the Kerr effect is balanced by the defocusing by the electron plasma created through multiphoton ionization. Loosely speaking, this equilibrium results in a type of "self-induced waveguide." In another description [7], the filament is a Bessel beam with an intensity distribution identical to that created by an axicon lens.

To understand qualitatively the difference between the two descriptions, one can use the stationary approach of Akhmanov [8–10], which starts with Maxwell's propagation equation, written for a continuous beam in the slowly varying envelope approximation and in cylindrical symmetry:

$$2i\partial_z \tilde{\mathscr{E}}_n = \frac{d^2\mathscr{E}_n}{d\chi^2} + \frac{1}{\chi}\frac{d\mathscr{E}_n}{d\chi} + \left|\mathscr{E}_n\right|^2\mathscr{E}_n - \frac{\gamma_k}{2}\mathscr{E}_n^{2K-2}\mathscr{E}_n. \quad (1)$$

In Eq. (1), the electric field of the light has been written as $E(t, z) = \frac{1}{2}\tilde{\mathscr{E}}(z)\exp(i\omega t - kz) + \text{c.c.}$, $\tilde{\mathscr{E}}_n =$

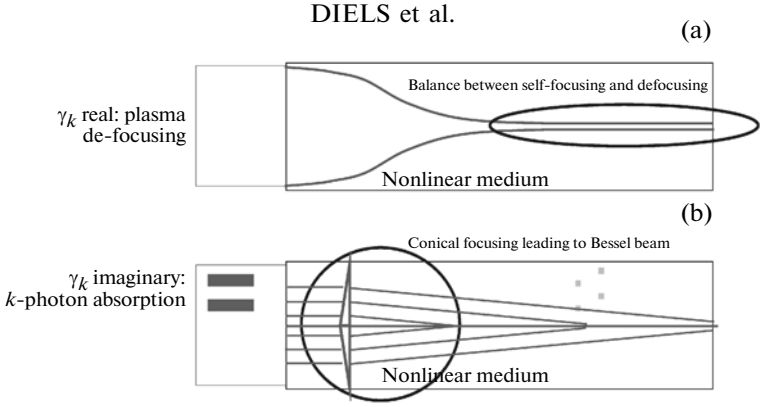

Fig. 1. Illustration of the interpretation of filaments according to (a) the self-induced waveguide model, and (b) the Bessel beam model. We start with a collimated beam entering the nonlinear medium (air). In (a), where γ_k in Eq. (1) is purely real, the beam is first focused by the Kerr nonlinearity, until it reaches a diameter where the plasma defocusing compensates the Kerr focusing, this latter region of "self-trapping" is shown in the blue ellipse. In (b), γ_k is purely imaginary. As the beam starts self-focusing, nonlinear multiphoton absorption also changes the intensity profile, which in turn changes the wavefront, resulting if an axicon-type lensing of the beam. The conical nonlinear focusing of the beam results in an intensity distribution on axis shaped as a Bessel function, hence the denomination "Bessel beam" for this type of filamentation.

$\tilde{\mathcal{E}}(z)/\mathcal{E}_0$ is the electric field complex envelope normalized to a field $\mathcal{E}_0 = \sqrt{\eta_0/n_2}$ (η_0 is the characteristic impedance of the medium, and $n_2 I = n_2 |\tilde{\mathcal{E}}(z)|^2/(2\eta_0)$ the nonlinear index of refraction). $\chi = kr$ is the radial coordinate r normalized to the wavelength. The higher order nonlinear term $\frac{\gamma_k}{2}\mathcal{E}_n^{2K-2}\mathcal{E}_n$ has been written in the form proposed by Dubietis et al. [7].

The above Eq. (1) can be used to explain the difference between the two major approaches to explain filamentation in air. The oldest version is that of a plasma channel, which corresponds to the coefficient γ_k being real; the last term of Eq. (1) representing a higher order contribution to the nonlinear index, resulting in self-de-focusing that balances the self-focusing effect. The filamentation results then from a balance between self-focusing due to the Kerr effect, and defocusing by the electron plasma created through multiphoton ionization. Loosely speaking, this equilibrium results in a type of "self-induced waveguide," as sketched in Fig. 1a. In the second model [7], the higher order coefficient γ_k is imaginary, representing multiphoton absorption. It has been shown [7] that, through the inclusion of this term, the propagation Eq. (1) leads to a conical phase-front, similar to the one created by axicon focusing. The k-vectors focus at successive points aligned along the beam axis, as sketched in Fig. 1b, resulting in a Bessel beam intensity distribution on axis [7, 11, 12].

It is worth mentioning that this "dilemma" between two models has been resolved in the case of self-focusing in solids and liquids in favor of the "Bessel beam model" [13]. Our results clearly indicate that the physics of filamentation is different in air.

3. DIAGNOSTIC METHOD

A major challenge in the study of filaments is to access experimentally the optical field of a filament. Any reliable measurement requires that the field be *linearly* attenuated. Otherwise, the nonlinearity of any window, solid state filter or material will dominate that of air. One solution is to use a plate of fused silica at grazing incidence. This was employed by other groups and was also used to observe the first UV filaments [14]. Unfortunately, the small fraction of the beam that is transmitted through the plate (6% for $\theta_i = 89°$) is still above the critical power for self-focusing in fused silica. The wavefront distortion and self-phase modulation can be minimized by using a thin plate ($\leq$1 mm). It is then however impossible to have the required flatness of $\lambda/10$ over the 10 cm diameter required for grazing incidence.

The solution that we introduce is a large rigid mirror with a maximum reflectivity coated at grazing incidence. We have found that a standard Nd:YAG high reflector coating (maximum reflectivity for s-polarization at normal incidence for 1.06 μm) has a transmission of less than 0.5×10^{-6} at 89° incidence. The transmitted light from a filament is sufficiently attenuated that nonlinear effects are negligible in the substrate. For UV filaments, a maximum reflectivity coating at normal incidence for 355 nm has also a transmission of less than 0.5×10^{-6} at 89° incidence.

The theoretical transmission curves have been verified for eight different wavelengths, at a grazing incidence of 88.5°. This method of attenuating the beam is limited to linearly s-polarized beams. Extra care had been taken to convert the output beam of the laser from p-polarization to s-polarization using waveplates and a high extinction ratio polarizer. Table lists the transmission factors (in percent) for the 1.064 total reflector at 89° incidence [14].

4. AERODYNAMIC WINDOW

The aerodynamic window is a novel diagnostic tool for the experimental study of filaments. A supersonic air flow creates a differential pressure in the aerodynamic window that effectively separates low-pressure vacuum chamber (below 400 Pa) from atmospheric pressure (10^5 Pa) on the outside. Since no optical element other than air is used, the intensity profile of the optical pulse launched in air can be controlled by linear optics. Also, any self-focusing or higher order nonlinearity is absent in the vacuum chamber prior to the formation of filaments. Thus, the onset of filamentation (boundary condition) can be well-defined using the aerodynamic window. The pressure distribution in the nozzle of the aerodynamic window is indicated in Fig. 2. The darker blue region indicates a pressure <5 mbar. The light yellow orange sections indicated a pressure in excess of 900 mbar.

5. EXPERIMENTS

Using these tools, we performed various experiments that should invalidate one of the two models plasma channels or Bessel beams. A 3-m focal distance lens is used in all experiments to initiate the focusing. We compared three different experimental situations:

(1) The beam is propagating all the way through the atmosphere—this is the conventional situation.

(2) The beam focusing process takes place in a vacuum. The beam is focused in vacuum to the approximate size of the filament, before being launched into the atmosphere, as shown in Fig. 2.

(3) A beam is focused in the atmosphere, and subsequently launched into vacuum.

Only the plasma channel model can explain filamentation in the situation (2) since there is no nonlinear "preparation" of the beam before a filament is formed in air. Only the Bessel beam model can explain filamentation in the situation (3), where there is no medium to create a waveguide.

5.1. Spectral Measurements

Our laser beam of 4 mm ($1/y^2$ radius or FWHM/1.177) is focused by a 3-m focal distance lens at the entrance of an aerodynamic window, creating a beam waist of 200 μm ($1/e^2$ radius). The combination of a grazing incidence plate and spectrometer are positioned at various distances from the geometrical focus of the lens (located at the entrance of the aerodynamic window). The spectra shown are corrected for the transmission function of the grazing incidence plate. The recorded spectra for the wavelength range around and above the central laser wavelength are shown in Fig. 3. One notices that, for the spectra corresponding to the filaments launched from vacuum (referred to as situation (2) in the previous section), there is very little

The theoretical percent transmission versus wavelength for the grazing incidence mirror for *s*- and *p*-polarized light (89° incidence)

λ, nm	% T_s	% T_p	λ, nm	% T_s	% T_p
780	0.000228	14.327976	800	0.000067	5.076257
781	0.000211	13.433172	801	0.000064	5.014465
782	0.000195	12.545672	802	0.000061	4.97625
783	0.000181	11.689771	803	0.000059	4.96135
784	0.000169	10.882014	804	0.000057	4.969877
785	0.000157	10.13233	805	0.000054	5.002339
786	0.000147	9.445485	806	0.000052	5.059672
787	0.000137	8.822507	807	0.000051	5.143288
788	0.000129	8.261913	808	0.000049	5.255144
789	0.000121	7.760668	809	0.000047	5.397834
790	0.000113	7.314895	810	0.000046	5.574713
791	0.000107	6.920375	811	0.000044	5.790063
792	0.000101	6.57287	812	0.000043	6.049313
793	0.000095	6.268338	813	0.000042	6.359335
794	0.00009	6.00305	814	0.000041	6.728845
795	0.000086	5.773655	815	0.00004	7.168937
796	0.000081	5.57721	816	0.000039	7.693832
797	0.0000775	.411182	817	0.000038	8.3219
798	0.000074	5.273442	818	0.000037	9.077097
799	0.00007	5.162253	819	0.000036	9.991006

generation of new frequencies in the IR portion of the spectrum, and little distortion of the original spectrum (Fig. 3a). The spectra taken at successive distances from the window are decreasing in intensity, most likely because of multiphoton ionization (consistent

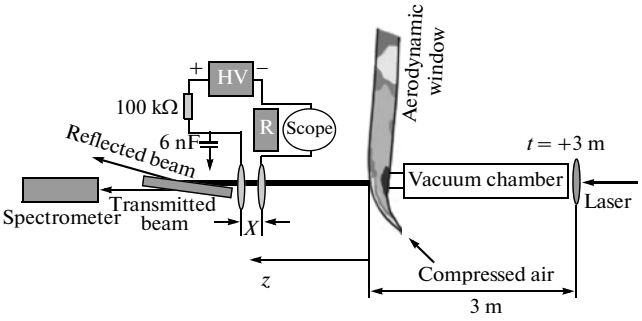

Fig. 2. The oscillator-amplifier system produces pulses of approximately 10 mJ energy and 200 fs duration, in a beam of $w = 4$ mm width. These pulses are focused by a 3 m focal length lens into a vacuum tube terminated by an aerodynamic window. The beam is incident at grazing incidence onto a large mirror with a maximum reflectivity coating designed for 1.064 nm at 0° incidence. The attenuated beam (attenuation factor ≈10^8) is then sent into a spectrometer. The nitrogen fluorescence at 337.1 nm and conductivity of the filament can be measured along the beam propagation.

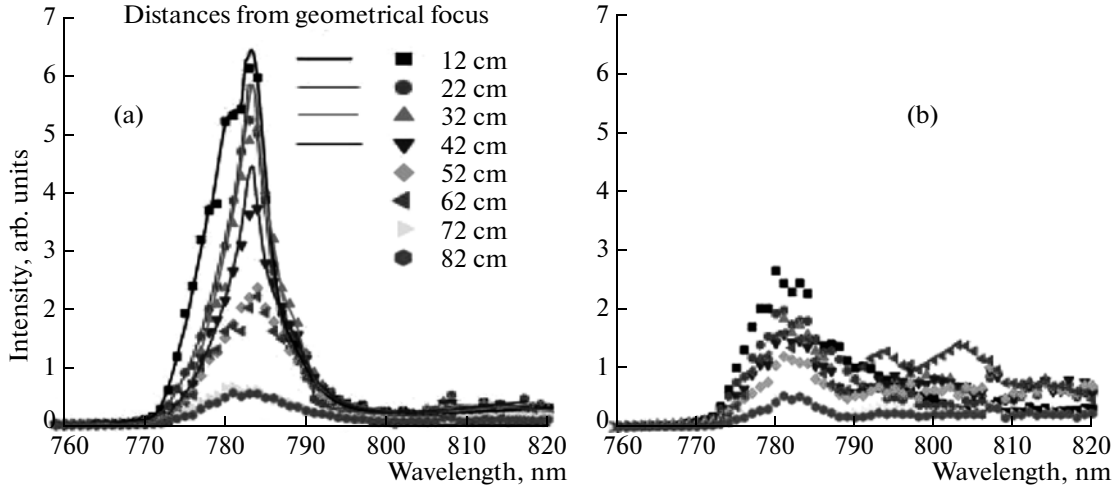

Fig. 3. Spectra recorded at various distances from the geometrical focus of the 3 m lens are displayed for the case of (a) focusing in vacuum (aerodynamic window on) and (b) focusing in air (aerodynamic window off).

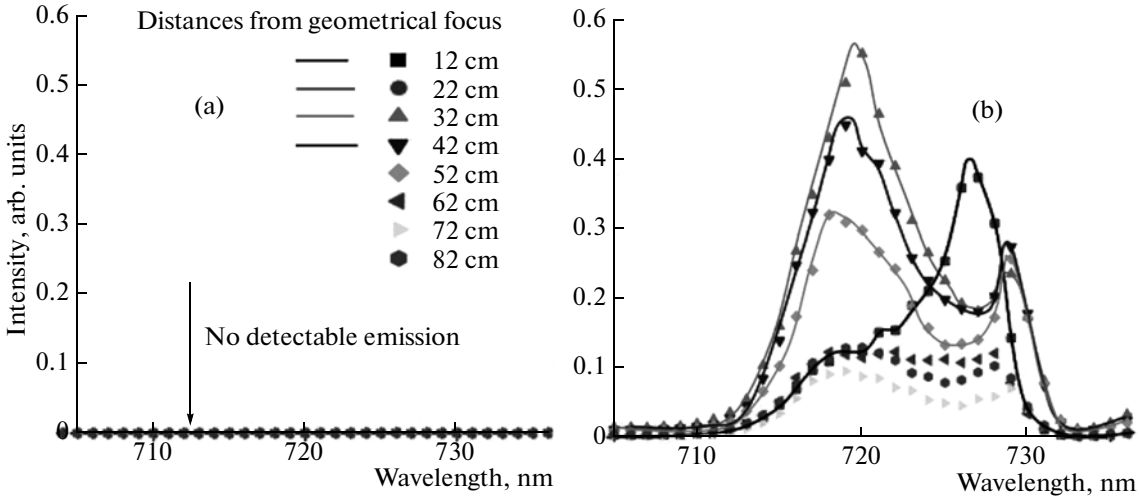

Fig. 4. New wavelengths generated in the blue region of the spectrum, recorded at various distances from the geometrical focus of the 3 m lens: (a) focusing in vacuum (aerodynamic window on) and (b) focusing in air (aerodynamic window off).

with the measurements of conductivity presented in Section 5.3). Profile measurements presented in Section 5.2 show the beam to remain confined for 70 cm.

The spectra issued from the filament prepared in air (referred to as situation (1) in the previous section) show considerably more attenuation, and generation of new frequencies in the IR. The contrast is more striking for the wavelength region shorter than that covered by the pulse spectrum, as shown in Fig. 4. For the case of the filament generated in air, new wavelengths are being generated (Fig. 4b). By contrast, when the filaments are generated from a focal spot in vacuum, no light is detected in the wavelength region between 700 and 740 nm (Fig. 4a).

One would be led to believe from these measurements that filaments are not generated when launched from a beam waist in vacuum. Measurements of filament profiles, plasma formation and conductivity presented below dispel completely this hasty conclusion: the filaments created through a waist as initial condition are the only real "self-induced waveguides."

5.2. Beam Profile—Filaments in Air, Created by Focusing in Air or in Vacuum

A beam expander followed by a CCD camera is placed after the linear attenuating plate. The "filament" size ($1/e^2$ radius) is plotted (Fig. 5) as a function of distance from the geometrical focus of the lens (colocated for these measurements at the entrance of the aerodynamic window). Linear diffraction of $w_0 =$ 200 μm Gaussian beam is indicated by the black solid

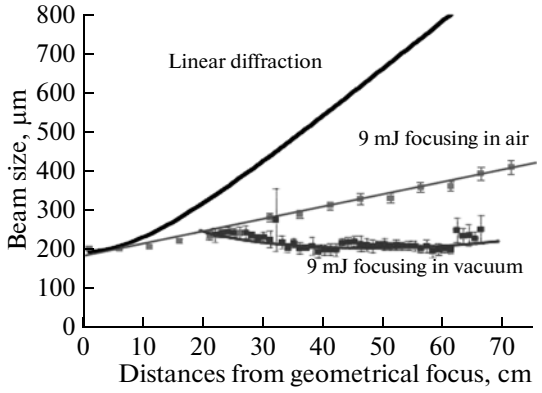

Fig. 5. Width of successive profile measurements taken at various distances from the aerodynamic window. At low energy, the profiles follow the linear diffraction theory curve (shown in black).

curve. A 9 mJ pulse focused in vacuum, and launched in air through the aerodynamic window, conserves its diameter over a distance of a little more than 70 cm. This observation is consistent with the self-induced waveguide model, even though no conical emission is observed, as indicated by Fig. 4.

In the case of the pulse focused in air, a similar confinement is observed, with a diameter increasing from 200 to 400 μm, before linear diffraction takes over.

5.3. Plasma Formation, Conductivity

For these measurements, the filament was made to pass through well-profiled holes in a pair of electrodes. The minimum breakdown voltage is measured as the filament passes through the holes. We have shown previously that the breakdown voltage is inversely proportional to the density of electrons deposited by the pulse [15]. The measurements show clearly that the plasma density generated is significantly less in the case of the filament prepared in air. The self breakdown raises from 8 to 15 kV in only 15 cm. In the case of the filaments prepared in vacuum, the self-breakdown increases from 9 to 14 kV over 40 cm. The larger plasma density, over a longer distance in the case of the filament prepared in vacuum, is in agreement with the beam profile measurements presented above.

Consistent with the formation of a plasma, there should be emission from the nitrogen ions at 337.1 nm due to the second positive system of N_2, which is indeed observed, as shown in the measurements presented in Fig. 6a. Next, a voltage *below breakdown* is applied between the electrodes, and a current is measured as the filament passes through the hole in the electrodes. The discharge current is plotted as a function of the distance to a fixed reference point (3 m from the lens, where the aerodynamic window is located), for various initial conditions, in Fig. 6a. The curves for filament prepared in air or in vacuum are displaced by approximately 20 cm, suggesting that the nonlinear focus starts 20 cm earlier in air. Both measurements in Fig. 6 are made with linear (solid lines) and circular (dashed lines) polarizations. A particularly interesting observation is the total absence of filamentation for circular polarization, in the case of the filament prepared in vacuum. This is in contrast to the case of filaments prepared in air, where the conductivity and nitrogen fluorescence are not much affected by the polarization of the beam. A possible explanation is that the conical emission, which is only observed in the case of the filaments produced in air, is the source of ionization in that particular situation. Even in the

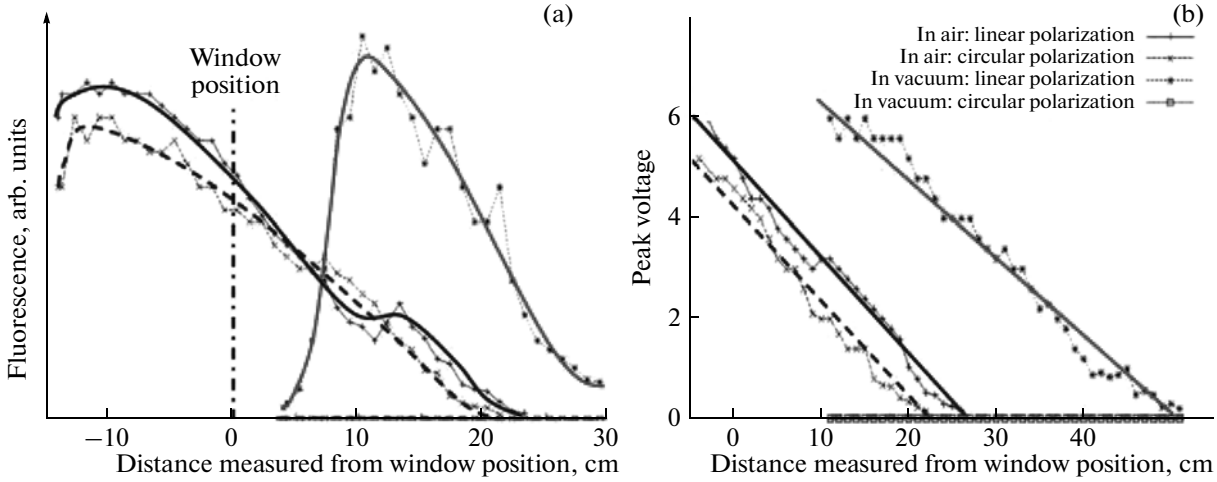

Fig. 6. Plasma parameters versus distance (in cm) to the geometrical focus of the 3 m focal distance lens, where the aerodynamic window is located. The solid lines correspond to linear polarization, the dashed lines to circular polarization. The red lines are for the filament generated from the beam waist in vacuum. The blue lines for the filament generated in air: (a) fluorescence, and (b) current. The current induced by the filament is measured across a 22 Ω resistance. The voltage applied to the electrodes is 4 kV (less than the lowest breakdown voltage).

case of circularly polarized beam, the conical emission created by four wave mixing may have a linear component.

More measurements and theoretical analysis are required to distinguish between these two origins for ionization. Measurement of the polarization of the conical emission created with a circularly polarized beam could shed some light into this problem.

6. CONCLUSIONS

In order to isolate the properties of filaments resulting from a balance between Kerr-lens self-focusing and plasma defocusing, we have focused a beam in vacuum, and launched it within the Rayleigh range into the atmosphere. Filaments produced by this technique do not exhibit any conical emission, which suggest that the spectral broadening and creation of new wavelengths takes place in the pre-filamentation stage.

The filaments created from a focal spot in vacuum propagate over longer distance than the single filaments prepared in air, and create a denser plasma over longer distance. A surprising result is that the plasma and the filament do not exist if the initial condition in vacuum is circularly polarized, in contrast to the situation of filaments prepared from a macroscopic beam in air.

These measurement confirm the mechanism of plasma confinement, but do not exclude the formation of a Bessel beam. In order to verify or infirm the "Bessel beam" theory, the filament should be prepared in air, and launched in vacuum. Preliminary measurements show that the beam profile versus distance in vacuum starts at a smaller diameter than the filament propagating in air. The diameter of the intensity profile remains constant for a shorter distance (≈30 cm) than in the case of the filament propagating in air.

REFERENCES

1. A. Braun, G. Korn, X. Liu, D. Du, J. Squier, and G. Mourou, "Self-channeling of High-peak-power fs Laser Pulses in Air," Opt Lett. **20**, 73–75 (1994).
2. Xin Miao Zhao, Patrick Rambo, and Jean-Claude Diels, "Filamentation of Femtosecond UV Pulses in Air," in **QELS 1995,** QThD2 (Opt. Soc. Am., Baltimore, MA, 1995), vol. 16, p. 178.
3. S. L. Chin, S. A. Hosseini, W. Liu, Q. Luo, F. Thberge, N. Aközbek, A. Becker, V. P. Kandidov, O. G. Kosareva, and H. Schroeder, "The Propagation of Powerful Femtosecond Laser Pulses in Optical Media: Physics, Applications, and New Challenges," Can. J. Phys. **83**, 863–905 (2005).
4. A. Couairon and A. Mysyrowicz, "Femtosecond Filamentation in Transparent Media," Phys. Rep. **441**, 49–189 (2007).
5. L. Bergé, S. Skupin, R. Nuter, J. Kasparian, and J. P. Wolf, "Ultrashort Filaments of Light in Weakly Ionized, Optically Transparent Media," Rep. Prog. Phys. **70**, 1633–1714 (2007).
6. V. P. Kandidov, S. A. Shlenov, and O. G. Kosareva, "Filamentation of High-power Femtosecond Laser Radiation," Opt. Lett. **39**, 205–228 (2009).
7. A. Dubietis, E. Gaisauskas, G. Tamosauskas, and P. Di Trapani, "Light Filaments without Self-channeling," Phys. Rev. Lett. **92**, 253903-1–253903-5 (2004).
8. S. A. Akhmanov, A. P. Sukhorukov, and R. V. Khokhlov, "Self Focusing and Self Trapping of Intense Light Beams in a Nonlinear Medium," Sov. Phys. JETP **23**, 1025–1033 (1966).
9. S. A. Akhmanov, A. P. Sukhorukov, and R. V. Khokhlov, "Development of an Optical Waveguide in the Propagation of Light in a Nonlinear Medium," Sov. Phys. JETP **24**, 198–201 (1967).
10. S. A. Akhmanov, V. A. Vysloukh, and A. S. Chirkin, *Optics of Femtosecond Laser Pulses* (AIP Press, 1991).
11. D. Faccio, A. Porras, A. Dubietis, F. Bragheri, A. Couairon, and P. Di Trapani, "Conical Emission, Pulse Splitting, and X-wave Parametric Amplification in Nonlinear Dynamics of Ultrashort Light Pulses," Phys. Rev. Lett. **96**, 193901 (2006).
12. D. Faccio, A. Averchi, A. Lottil, P. Di Trapani, A. Couairon, D. Papazoglou, and S. Tzortzakis, "Ultrashort Laser Pulse Filamentation from Spontaneous X-Wave Formation in Air," Opt. Express **16**, 1565–1570 (2008).
13. E. Gaizauskas, A. Dubietis, V. Kudriasov, V. Sirutkaitis, A. Couairon, D. Faccio, and Paolo Di Trapani, "On the Role of Conical Waves in Self-focusing and Filamentation of Femtosecond Pulses with Nonlinear Losses," in *Self-Focusing, Past and Present*, Ed. by M. Bass (Springer, Berlin, Heidelberg, 2009), pp. 457–479.
14. Olivier J. Chalus, A. Sukhinin, A. Aceves, and J.-C. Diels, "Propagation of Non-diffracting Intense Ultraviolet Beams," Opt. Commun. **281**, 3356–3360 (2008).
15. P. K. Rambo, J. Schwarz, and J. C. Diels, "High Voltage Electrical Discharges Induced by an Ultrashort Pulse UV Laser System," J. Opt. A **3**, 146–158 (2001).